ResearchGate

See discussions, stats, and author profiles for this publication at: https://www.researchgate.net/publication/252640269

Morkovin Hypothesis and the Modeling of Wall-Bounded Compressible Turbulent Flows

Article *in* AIAA Journal · September 1998

DOI: 10.2514/2.584

CITATIONS
22

READS
702

3 authors, including:

R.M.C. So
The Hong Kong Polytechnic University
419 PUBLICATIONS **6,167** CITATIONS
SEE PROFILE

T. B. Gatski
207 PUBLICATIONS **8,396** CITATIONS
SEE PROFILE

Some of the authors of this publication are also working on these related projects:

Lattice Boltzmann Method View project

Temporal Large-Eddy Simulation (TLES) View project

All content following this page was uploaded by R.M.C. So on 27 May 2014.

The user has requested enhancement of the downloaded file.

AIAA JOURNAL
Vol. 36, No. 9, September 1998

Morkovin Hypothesis and the Modeling of Wall-Bounded Compressible Turbulent Flows

R. M. C. So*
Hong Kong Polytechnic University, Hong Kong
T. B. Gatski†
NASA Langley Research Center, Hampton, Virginia 23681
and
T. P. Sommer‡
ABB Power Generation, Ltd., 5401 Baden, Switzerland

Modeling of compressible wall-bounded turbulent flows relies on the hypothesis of Morkovin, who suggested that compressibility effects on turbulence could be accounted for by the mean density variations alone. This hypothesis has been shown to yield good results for the mean velocity and mean temperature fields when the incompressible turbulence models are extended directly to calculate compressible turbulent boundary layers. However, its applicability for the turbulence field has been less closely scrutinized. The reason is the lack of sufficiently detailed compressible turbulence data for comparison. Such data are now becoming available. Therefore, the purpose here is to assess the applicability of the Morkovin hypothesis to the turbulence field using direct numerical simulation data of a supersonic, flat plate boundary layer. A near-wall Reynolds-stress closure based on a quasi-linear pressure-strain model is used to calculate this supersonic, boundary-layer flow. Comparisons between calculations and direct numerical simulation data show that the Morkovin hypothesis is just as applicable for the turbulence field and there is a dynamic similarity between the near-wall turbulence field of an incompressible and a compressible wall-bounded turbulent flow. In addition, the validation of this model is reported for compressible flow calculations covering a wide range of Mach numbers with adiabatic and constant-temperature wall boundary conditions. These results show that the model yields good predictions of flat-plate turbulent boundary layers up to a Mach number of 10.31.

Introduction

TURBULENCE modeling plays an important role in computational fluid dynamics, which is used extensively as a tool in the design of advanced aircraft. These aircraft are usually designed to fly at supersonic speeds, and associated with the advanced designs, a host of new problems such as shock/boundary-layer interactions with turbulence amplification and flow separation occur. Not much is known about these flow problems, particularly the physics of wall-bounded and separated compressible turbulence. A knowledge of the near-wall flow is of crucial importance if these flows are to be predicted. This, in turn, depends on the ability to model compressible turbulent boundary-layer flows. To model near-wall compressible turbulent flows correctly, an asymptotically correct near-wall incompressible turbulence model has to be formulated first. A fairly complete review of incompressible models has been given by So et al.[1] Altogether, eight models were reviewed. The models discussed were quite similar in that they were based on the high-Reynolds-number pressure-strain model of Launder et al.[2] or its variations. Some models were not asymptotically correct because they were formulated to satisfy the exact wall boundary conditions for the Reynolds stresses only.[3,4] Others failed to predict the anisotropy of the normal stresses near a wall.[5] Still others failed to give a correct behavior for the dissipation rate of k, the turbulent kinetic energy, near a wall.[6–8]

A careful examination of the failures of these models and the available experimental and direct numerical simulation (DNS) data[9–15] reveals that several characteristics should be present in a near-wall model if it is to replicate the turbulence statistics correctly. First and foremost is the gradual disappearance of the influence of the near-wall corrections. However, this condition is not entirely satisfied by existing models.[1] As a result, the von Kármán constant is calculated incorrectly and found to depend on the Reynolds number, which is not consistent with experimental and DNS data.[16] Second, the predicted behavior of the dissipation rate of k should have the right trend compared with DNS data. Third, the model should yield the correct near-wall asymptotes for the Reynolds stresses. Because existing near-wall models fail to predict some or all of these characteristics correctly, an alternative near-wall model has to be sought. One such model has recently been put forward.[17] This model is based on the quasi-linear pressure-strain (SSG) model,[18] which has been shown to yield the logarithmic law of the wall correctly without the use of pressure reflection terms even when wall functions are invoked.[19] The model has been validated against a wide variety of experimental and DNS data with vastly different Reynolds number and has been demonstrated to best reproduce the aforementioned characteristics and the effects of Reynolds number.[17,20] Therefore, this near-wall model[17] appears to be a good candidate for extension to compressible flows.

The extension to compressible flows is quite straightforward if the Morkovin hypothesis[21] can be invoked and the equations are written in terms of Favre-averaged variables. This hypothesis allows for the use of variable density extensions of existing incompressible turbulence models to compressible turbulence. For compressible turbulence, it is further suggested that the dissipation rate ε could be decomposed into a solenoidal part ε_s and a compressible part ε_c so that $\varepsilon = \varepsilon_s + \varepsilon_c$ (Ref. 22). The solenoidal dissipation rate is associated with the energy cascade; therefore it approaches the incompressible limit correctly. In view of this and consistent with the Morkovin hypothesis, ε_c is neglected in most formulations and ε is taken to be given by ε_s alone. These two approximations together imply that the turbulence statistics are only altered by compressibility effects through changes in the mean density. The soundness of these assumptions for the mean field has recently been demonstrated by a number of studies that essentially verify their validity over a

Received Oct. 21, 1997; revision received May 2, 1998; accepted for publication May 18, 1998. Copyright © 1998 by the authors. Published by the American Institute of Aeronautics and Astronautics, Inc., with permission.

*Chair Professor and Head, Department of Mechanical Engineering, Hung Hom, Kowloon.
†Senior Research Scientist, Flow Physics Branch.
‡Research Scientist, Gas Turbine Group.

freestream Mach number M_∞ range of 2.24–10.31 with adiabatic as well as constant temperature wall boundary conditions.[23–28] However, their validity for the turbulence field has not been adequately demonstrated. The conventional wisdom is that, if the hypothesis is valid for the mean field, it could be assumed to be equally valid for the turbulence field.[23–28] Also, the asymptotic analyses[17] used to deduce the near-wall corrections for the Reynolds-stress equations are carried out for incompressible flows only. Their extension to compressible flows needs verification.

Up to now, detailed turbulence statistics have not been used to justify the application of the Morkovin hypothesis to the modeling of a compressible turbulence field. This is partly due to the lack of credible measurements of compressible turbulence near a wall, which are extremely difficult to obtain. With advances made in DNS of incompressible turbulence, it is now possible to simulate spatially evolving, compressible turbulent flows at $Re_\theta = U_\infty \theta / v_\infty$ of approximately 5.4×10^3 (Ref. 29), where U_∞ is the freestream velocity, θ is the momentum thickness, and v_∞ is the freestream kinematic viscosity. Because the near-wall turbulence model[17] has been shown to be valid for wall-bounded flows with low as well as high Reynolds numbers, its extension to compressible flows would be best verified using the most recent DNS data[29] on supersonic turbulent boundary layers. Therefore, for the first time, the applicability of the Morkovin hypothesis to the turbulence field could be examined in detail and its validity assessed.

There are three objectives in the present study: 1) to assess the validity of the Morkovin hypothesis for the compressible turbulence field; 2) to examine the extension of the incompressible asymptotic analyses to compressible flows and, hence, indirectly to establish the dynamic similarity behavior of the incompressible and compressible turbulence field near a wall; and 3) to verify the general validity of the near-wall Reynolds-stress model for compressible wall-bounded turbulent flows with a wide range of M_∞ and adiabatic as well as constant-temperature wall boundary conditions. These objectives are accomplished by comparing the model calculations with the recently obtained DNS data of a compressible boundary layer at $M_\infty = 2.25$ on an adiabatic wall[29] and other experimental measurements at M_∞ varying from 2.87 to more than 10 with thermal boundary conditions given by adiabatic and constant temperature walls.[30–35]

Mean Flow Equations

For compressible turbulent flows, the mass, momentum, and energy equations are usually written in terms of Favre-averaged quantities where a density-weighted average is used to decompose the fluctuating quantities, besides pressure and density, into a mass-weighted mean part and a mass-weighted fluctuating part. On the other hand, the pressure and density are decomposed using a Reynolds average, which results in a Reynolds-averaged mean part and a Reynolds-averaged fluctuating part. For any variable F, the mass-weighted mean is denoted by $\tilde{F}$, the mass-weighted fluctuating part by f, the Reynolds-averaged mean by $\bar{F}$, and the Reynolds-averaged fluctuating part by f'. The fluid density is taken to be ρ, the dynamic viscosity μ, the thermal conductivity k_t, the pressure p, the velocity vector U_i, the temperature Θ, the specific heat at constant pressure C_p, and the gas constant R. Neglecting real gas effects, bulk viscosity, and body forces, one can express these mean flow equations in Cartesian tensor form for an ideal gas as

$$\partial_t \bar{\rho} + (\bar{\rho}\tilde{U}_i)_{,i} = 0 \tag{1}$$

$$\partial_t(\bar{\rho}\tilde{U}_i) + (\bar{\rho}\tilde{U}_i\tilde{U}_j)_{,j} = -\bar{P}_{,i} - \tfrac{2}{3}(\bar{\mu}\tilde{U}_{j,j})_{,i} + [\bar{\mu}(\tilde{U}_{i,j} + \tilde{U}_{j,i})]_{,j} - (\bar{\rho}\tau_{ij})_{,j} \tag{2}$$

$$\partial_t(\bar{\rho}\tilde{C}_p\tilde{\Theta}) + (\bar{\rho}\tilde{U}_i\tilde{C}_p\tilde{\Theta})_{,i} = \partial_t\bar{P} + \tilde{U}_i\bar{P}_{,i} + \bar{u}_i\bar{P}_{,i} + \overline{u_i'p_{,i}'} + \bar{\sigma}_{ij}\tilde{U}_{i,j} + \bar{\sigma}_{ij}\bar{u}_{i,j} + \bar{\rho}\varepsilon - (\bar{\rho}\tilde{C}_pQ_i)_{,i} + (\bar{k}_t\tilde{\Theta}_{,i})_{,i} \tag{3}$$

$$\bar{P} = \bar{\rho}R\tilde{\Theta} \tag{4}$$

where ∂_t is the time derivative, $(\cdot)_{,i}$ denotes a gradient with respect to the spatial coordinate x_i, the Einstein summation convention applies to repeated indices, and the kinematic Reynolds-stress tensor, the Reynolds-heat-flux vector, and the turbulent dissipation rate are defined as $\tau_{ij} = \widetilde{u_iu_j}$, $Q_i = \widetilde{u_i\theta}$, and $\bar{\rho}\varepsilon = \sigma_{ij}'u_{i,j}'$, respectively. From this point on, the symbol ε is taken to mean either the true dissipation rate in incompressible flow or ε_s in compressible flows. The mean viscous stress tensor is given by

$$\bar{\sigma}_{ij} = -\tfrac{2}{3}\bar{\mu}\tilde{U}_{k,k}\delta_{ij} + \bar{\mu}(\tilde{U}_{i,j} + \tilde{U}_{j,i}) \tag{5}$$

Additional assumptions are made in the course of deriving Eqs. (1–5), and these are the neglect of turbulent fluctuations of the dynamic viscosity, the thermal conductivity, and the specific heats. Also, the velocity-pressure gradient correlation $\overline{u_i'p_{,i}'}$ can be written in the equivalent form[23] as

$$\overline{u_i'p_{,i}'} = -(\bar{\rho}R\tilde{\Theta}\bar{u}_i)_{,i} + (\bar{\rho}R\widetilde{u_i\theta})_{,i} - \overline{p'u_{i,i}'} \tag{6}$$

From these equations, it can be seen that, to achieve closure, models are required for τ_{ij}, Q_i, ε, the pressure dilatation correlation $\overline{p'u_{i,i}'}$, and the mass flux vector $\bar{u}_i$. The near-wall Reynolds-stress model[17] is extended to compressible flows by invoking the Morkovin hypothesis. Therefore, it is justified to neglect $\overline{p'u_{i,i}'}$ and $\bar{u}_i$ in the modeling of supersonic turbulent flows. Gradient transport is assumed for Q_i so that $-Q_i = -\widetilde{u_i\theta} = (v_t/Pr_t)(\partial\tilde{\Theta}/\partial x_i)$, where v_t is the eddy viscosity defined by $v_t = -\widetilde{uv}/(\partial\tilde{U}/\partial y)$, $Pr_t = 0.9$, and y is the normal coordinate. Because the present objective is to assess the appropriateness of the Morkovin hypothesis, this assumption for the turbulent heat flux is acceptable. As will be seen in the next section, heat flux modeling does not affect the calculations of the Reynolds stresses directly other than to influence the determination of the mean density. The same is also true of Eqs. (1–3). Therefore, a lower-level heat flux model is still appropriate. One point to note is that, when v_t is evaluated numerically, modifications are made to avoid division by zero near the edge of the boundary layers.

Modeled Reynolds-Stress Equations

The compressible Reynolds-stress equation written in the same form as its incompressible counterpart is given by

$$\partial_t(\bar{\rho}\tau_{ij}) + (\tilde{U}_k\bar{\rho}\tau_{ij})_{,k} = \bar{\rho}D^v_{ijk,k} + \bar{\rho}C_{ijk,k} + \bar{\rho}P_{ij} + \bar{\rho}\Pi^d_{ij} - \bar{\rho}\varepsilon_{ij} + \bar{\rho}\Pi^{dl}_{ij} + \bar{\rho}M_{ij} \tag{7}$$

where $\bar{\rho}D^v_{ijk,k} = (\overline{u_i'\sigma_{jk}'} + \overline{u_j'\sigma_{ik}'})_{,k}$ and $\bar{\rho}C_{ijk,k} = -(\bar{\rho}\widetilde{u_iu_ju_k} + \overline{p'u_i'}\delta_{jk} + \overline{p'u_j'}\delta_{ki})_{,k}$ are the viscous and turbulent diffusion tensors, respectively; $\bar{\rho}P_{ij} = (-\bar{\rho}\tau_{ik}\tilde{U}_{j,k} - \bar{\rho}\tau_{jk}\tilde{U}_{i,k})$ is the production tensor;

$$\bar{\rho}\Pi^d_{ij} = (\overline{p'u_{i,j}'} + \overline{p'u_{j,i}'}) - 2(\overline{p'u_{k,k}'}\delta_{ij})/3$$

and

$$\bar{\rho}\Pi^{dl}_{ij} = -2(\overline{p'u_{k,k}'}\delta_{ij})/3$$

are the pressure strain-rate and dilatation tensors, respectively; $\bar{\rho}\varepsilon_{ij} = \overline{\sigma_{ik}'u_{j,k}'} + \overline{\sigma_{jk}'u_{i,k}'}$ is the viscous dissipation rate tensor; and $\bar{\rho}M_{ij} = \bar{u}_i(\bar{\sigma}_{jk,k} - \bar{P}_{,j}) + \bar{u}_j(\bar{\sigma}_{ik,k} - \bar{P}_{,i})$ is the mass flux variation tensor. The last two terms in Eq. (7) arise as a result of compressibility and are identically zero for incompressible flows. Therefore, if the Morkovin hypothesis is invoked, the last two terms in Eq. (7) should be neglected and the turbulent diffusion, viscous dissipation, and pressure strain-rate correlation terms could be modeled as in constant-density flows. Consistent with this assumption, the term $\overline{p'u_{i,i}'}$ in Eq. (6) is also neglected. Finally, the viscous diffusion tensor $\bar{\rho}D^v_{ijk,k}$ is approximated by $(\bar{\mu}\tau_{ij,k})_{,k}$. Thus simplified, Eq. (7) can be closed by extending the incompressible near-wall model[17] to compressible flows. Without derivation, the models for the various terms can be generalized as

$$C_{ijk,k} = [C_s(k/\varepsilon)(\tau_{kl}\tau_{ij,l} + \tau_{jl}\tau_{ki,l} + \tau_{il}\tau_{jk,l})]_{,k} \tag{8}$$

$$\Pi^d_{ij} = \Pi^*_{ij} + \Pi^w_{ij} \tag{9}$$

$$\varepsilon_{ij} = \tfrac{2}{3}\varepsilon\delta_{ij} + \varepsilon^w_{ij} \tag{10}$$

Here, Π_{ij}^{*} is given by the high-Reynolds-numbermodel of Speziale et al.,[18] and Π_{ij}^{w} and ε_{ij}^{w} are near-wall corrections. The models for these terms can now be written for compressible flows as

$$\Pi_{ij}^{*} = -\left(2C_1\varepsilon + C_1^{*}\tilde{P}\right)b_{ij} + C_2\varepsilon\left(b_{ik}b_{kj} - \tfrac{1}{3}\Pi\delta_{ij}\right) - \alpha_1\left(P_{ij} - \tfrac{2}{3}\tilde{P}\delta_{ij}\right) - \beta_1\left(D_{ij} - \tfrac{2}{3}\tilde{P}\delta_{ij}\right) - 2\left[\gamma_1 + \left(C_3^{*}/2\right)\Pi^{\frac{1}{2}}\right]kS_{ij} \tag{11}$$

$$\Pi_{ij}^{w} = f_{w1}\left[\left(2C_1\varepsilon + C_1^{*}\tilde{P}\right)b_{ij} - C_2\varepsilon\left(b_{ik}b_{kj} - \tfrac{1}{3}\Pi\delta_{ij}\right) + \alpha^{*}\left(P_{ij} - \tfrac{2}{3}\tilde{P}\delta_{ij}\right) + 2\gamma^{*}kS_{ij}\right] + \Pi_{ij}^{p} \tag{12}$$

$$\Pi_{ij}^{p} = -\frac{1}{3}\left[\frac{\partial}{\partial x_l}\left(\bar{v}\frac{\partial\overline{u_iu_k}}{\partial x_l}\right)n_kn_j + \frac{\partial}{\partial x_l}\left(\bar{v}\frac{\partial\overline{u_ju_k}}{\partial x_l}\right)n_kn_i\right] + \frac{1}{3}\frac{\partial}{\partial x_m}\left(\bar{v}\frac{\partial\overline{u_ku_l}}{\partial x_m}\right)n_kn_ln_in_j \tag{13}$$

$$\varepsilon_{ij}^{w} = f_{w1}\left[-\frac{2}{3}\varepsilon\delta_{ij} + \frac{\varepsilon}{k}\frac{(\tau_{ij} + \tau_{ik}n_kn_j + \tau_{jk}n_kn_i + n_in_j\tau_{kl}n_kn_l)}{(1 + 3\tau_{kl}n_kn_l/2k)}\right] \tag{14}$$

where $D_{ij} = -(\tau_{ik}\tilde{U}_{k,j} + \tau_{jk}\tilde{U}_{k,i})$, $S_{ij} = (\tilde{U}_{i,j} + \tilde{U}_{j,i})/2$, $k = \tau_{ii}/2$ is the turbulent kinetic energy, $\tilde{P} = P_{ii}/2$, and the turbulent Reynolds number is defined as $Re_t = k^2/\bar{v}\varepsilon$. Finally, the anisotropic tensor b_{ij} and the damping function are given by $b_{ij} = (\overline{u_iu_j} - 2k\delta_{ij}/3)/2k$ and $f_{w1} = \exp[-(Re_t/200)^2]$, respectively.

The dissipation rate ε is assumed to be approximately equal to ε_s whose modeled equation, similar to its incompressible counterpart, can be written for compressible flows as

$$\partial_t(\bar{\rho}\varepsilon) + (\bar{\rho}\varepsilon\tilde{U}_k)_{,k} = (\bar{\mu}\varepsilon_{,k})_{,k} + [C_\varepsilon\bar{\rho}(k/\varepsilon)\tau_{ki}\varepsilon_{,i}]_{,k} + C_{\varepsilon1}(\varepsilon/k)\bar{\rho}\tilde{P} - C_{\varepsilon2}(\bar{\rho}\varepsilon\tilde{\varepsilon}/k) + \bar{\rho}\xi \tag{15}$$

A generalization of the near-wall correcting function ξ for compressible flows is given by

$$\xi = f_{w2}[-L(\varepsilon/k)\tilde{P} + M(\tilde{\varepsilon}^2/k) - N(\varepsilon\tilde{\varepsilon}/k)] \tag{16}$$

In Eq. (16), $\tilde{\varepsilon}$ and $\bar{\varepsilon}$ are defined by $\tilde{\varepsilon} = \varepsilon - 2\bar{v}(\partial\sqrt{k}/\partial x_2)^2$ and $\bar{\varepsilon} = \varepsilon - 2\bar{v}k/x_2^2$, respectively, and the damping function is given by $f_{w2} = \exp[-(Re_t/40)^2]$. Finally, the boundary conditions for the mean and turbulent velocity field are given by

$$\tilde{U}_i = k = \tau_{ij} = 0, \qquad \varepsilon_w = 2\bar{v}_w\left(\frac{\partial\sqrt{k}}{\partial y}\right)^2 \tag{17}$$

where y is the wall normal coordinate. The model constants are all taken to be the same as those given for the near-wall SSG model.[17] They are quoted here for reference: $C_1 = 1.7$, $C_2 = 4.2$, $C_1^{*} = 1.8$, $C_3^{*} = 1.3$, $\alpha_1 = 0.4125$, $\beta_1 = 0.2125$, $\gamma_1 = 0.01667$, $C_\varepsilon = 0.12$, $C_{\varepsilon1} = 1.50$, $C_{\varepsilon2} = 1.83$, $\alpha^{*} = -0.29$, $\gamma^{*} = 0.065$, $L = 2.25$, $M = 0.5$, and $N = 0.57$.

Results and Discussion

The boundary-layercode of Anderson and Lewis[36] is modified for the present calculations. A nonuniform grid with 101 points in the wall normal direction is used, and the boundary layer is calculated to the same Re_θ as the data set where comparisons with data are carried out. Therefore, the results are free of inlet condition effects when Re_θ is relatively large. Furthermore, the question of transition does not have to be addressed when comparisons are made at a given Re_θ. Comparisons of turbulence statistics are made solely with the DNS data set.[29] To draw conclusions on the appropriateness of the asymptotic analyses and the validity of the Morkovin hypothesis for the turbulence field, a comparison of the turbulence field for both incompressible and compressible turbulent flat plate boundary layers is desirable. Two sets of reliable incompressible data are selected for this purpose; one is a set of DNS data,[10] and the other is a set of experimental measurements.[11] The corresponding Re_θ for these two sets of data are 1.41×10^3 and 2.42×10^3, respectively, and bracket the reduced Re_θ of the DNS compressible flat plate boundary-layer data.[29]

Comparisons with measurements, on the other hand, are made with the measured mean velocity, mean temperature, and C_f only. In compressible boundary layers over adiabatic walls, the mean temperature profiles are not measured separately. Rather, they are interpreted from the mean velocity profiles by assuming the total enthalpy across the boundary layer to be constant. As a result, the temperature comparisons are not very meaningful for the flow cases with an adiabatic wall. From the measured mean velocity profiles, the von Kármán constant can be determined depending on whether the mean velocities are reduced in the conventional way[37] or by invoking the van Driest transformation.[38] Two von Kármán constants are deduced, and they are denoted by κ and κ_c for the conventional way and the van Driest transformation, respectively.

The conventional law of the wall[37] for compressible boundary layers can be deduced by invoking the Morkovin hypothesis,[21] the dimensional arguments of Millikan,[39] and the assumption of an overlap between the inner and outer layers. The result is given by

$$U^{+} = \frac{1}{\kappa(M_\tau, B_q, \gamma)}\ln y_w^{+} + B(B_q, M_\tau, \gamma, Pr_w) \tag{18}$$

where $u_\tau = (\tau_w/\rho_w)^{1/2}$, $y_w^{+} = yu_\tau/v_w$, $B_q = Q_{\text{tot}}/(\rho_w C_p u_\tau \tilde{\Theta}_w)$, $M_\tau = u_\tau/a_w$, $Pr_w = (C_p\mu_w)/k_w$, a_w is the sound speed evaluated at the wall, and $\gamma = (C_p/C_v)_w$ is the ratio of the specific heats evaluated at the wall. Here, the subscript w is used to denote values evaluated at the wall, Q_{tot} is the total heat transfer rate, and k_w is the fluid thermal conductivity evaluated at the wall. The von Kármán constant κ is parametric in M_τ, B_q, and γ, whereas the intercept is not only parametric in these variables but also the Prandtl number evaluated at the wall, Pr_w. On the other hand, according to van Driest,[38] the law of the wall for compressible boundary layers can be written as

$$U_c^{+} = \frac{U_c}{u_\tau} = \frac{1}{u_\tau}\int_0^{\tilde{U}}\left(\frac{\bar{\rho}}{\rho_w}\right)^{\frac{1}{2}}\mathrm{d}\tilde{U} = \frac{1}{\kappa_c}\ln y_w^{+} + B_c \tag{19}$$

Here, κ_c is the corresponding von Kármán constant and U_c is the transformed mean velocity. In Eq. (19), B_c is the intercept; however, unlike B in Eq. (18), its parametric dependence is not entirely clear. The determinations of κ and κ_c are compared in Table 1, where, in addition, the various measured and calculated C_f are compared. Note that the van Driest transformation is just another way of looking at compressible boundary layers. The validity and extent of this transformation has not been fully verified in the past. Therefore, it would be beneficial to compare this scaling argument with the more traditional approach for the compressible boundary-layercases considered here.

Altogether six different flow cases are selected to test the models. They are the heated wall case[35] where $M_\infty = 2.87$ and $\tilde{\Theta}_w/\Theta_{aw} = 1.10$, the DNS case[29] where $M_\infty = 2.25$ and $\tilde{\Theta}_w/\Theta_{aw} = 1.0$, the adiabatic wall cases[30,31] collected in Ref. 33 where $M_\infty = 4.54$ and 10.31 and $\tilde{\Theta}_w/\Theta_{aw} = 1.0$, the slightly cooled wall case[32] where $M_\infty = 5.29$ and $\tilde{\Theta}_w/\Theta_{aw} = 0.92$, and the high M_∞, highly cooled wall case[34] where $M_\infty = 8.18$ and $\tilde{\Theta}_w/\Theta_{aw} = 0.30$. Here, Θ_w is the wall temperature and Θ_{aw} is the adiabatic wall temperature. Not all of the results are shown; only selected cases are presented. However, all measured and calculated C_f, κ, and κ_c are compared in Table 1.

Turbulence Field Validation

The turbulence statistics near a wall can be expanded in terms of y. For incompressible flows, the near-wall variables are the friction velocity and the normal distance from the wall.[17] Furthermore, according to the Morkovin hypothesis, compressibility effects can be accounted for by the mean density variations alone. Therefore, this suggests that inner layer similarity between incompressible and compressible flows can be compared if the near-wall variables are defined by including the mean density and made dimensionless by the fluid properties evaluated at the wall. Denoting $k^{+} = \bar{\rho}k/\rho_w u_\tau^2$; $uv^{+} = \bar{\rho}\widetilde{u''v''}/\rho_w u_\tau^2$; $\varepsilon^{+} = \bar{\rho}\varepsilon v_w/\rho_w u_\tau^4$; and u', v',

Table 1 Comparison of the calculated and measured k, k_c, and $C_f \times 10^3$

				Experimental/DNS data				Model calculation		
Reference	$\tilde{\Theta}_w/\tilde{\Theta}_{aw}$	M_∞	Re_θ	κ	κ_c	$C_f \times 10^3$	M_g	κ	κ_c	$C_f \times 10^3$
34	0.3	8.18	4.6×10^3	0.35	0.29	0.98	0.52	0.40	0.28	1.05
32	0.92	5.29	3.936×10^3	0.48	0.34	1.31	0.28	0.44	0.29	1.12
31	1.0	10.31	1.5074×10^4	0.54	0.28	0.24	0.21	0.58	0.29	0.20
30	1.0	4.54	5.32×10^3	0.41	0.28	1.26	0.28	0.41	0.29	1.18
29	1.0	2.25	5.4×10^3	0.43	0.41	2.20	0.17	0.41	0.41	2.10
11	1.0	0	2.42×10^3	0.41	——	3.54	0	0.41	——	3.63
10	1.0	0	1.41×10^3	0.41	——	4.10	0	0.41	——	4.01
35	1.11	2.87	8.3899×10^4	0.52	0.37	1.10	0.13	0.51	0.35	1.15

and $w' = (\bar{\rho}\widetilde{u^2}/\rho_w u_\tau^2)^{1/2}$, $(\bar{\rho}\widetilde{v^2}/\rho_w u_\tau^2)^{1/2}$, and $(\bar{\rho}\widetilde{w^2}/\rho_w u_\tau^2)^{1/2}$, respectively, the expansions for the turbulence statistics in terms of $y^+ = y_w^+ = y u_\tau / v_w$ can be written as

$$k^+ = a_k y^{+2} + b_k y^{+3} + \cdots \tag{20a}$$

$$uv^+ = a_{uv} y^{+3} + b_{uv} y^{+4} + \cdots \tag{20b}$$

$$\varepsilon^+ = 2a_k + 4b_k y^+ + \cdots \tag{20c}$$

$$u' = a_u y^+ + b_u y^{+2} + \cdots \tag{20d}$$

$$v' = a_v y^{+2} + b_v y^{+3} + \cdots \tag{20e}$$

$$w' = a_w y^+ + b_w y^{+2} + \cdots \tag{20f}$$

where a_i and b_i are coefficients in the expansions for k^+, uv^+, u', v', and w'. Here, y^+ is also used to denote y_w^+ for compressible wall-bounded flows. Therefore, the ratios $k^+/\varepsilon^+ y^{+2}$ and $(a_u^2 + a_v^2 + a_w^2)/a_k$ are exactly $\frac{1}{2}$ and 2, respectively, at the wall, and u' and w' vary linearly with y^+, whereas v' and k^+ vary quadratically with y^+. At the wall, ε^+ is a constant. In all previous calculations of incompressible flows,[17] the ratios $k^+/\varepsilon^+ y^{+2} = \frac{1}{2}$ and $(a_u^2 + a_v^2 + a_w^2)/a_k = 2$ are recovered correctly. This means that the near-wall Reynolds-stress model is internally consistent and asymptotically correct for incompressible internal and external flows. Therefore, any deviation from these values is an indication of the inadequacy of the near-wall model. The present objectives are to show that expansions (20) are also applicable for compressible flows, which then verifies that there is indeed a dynamic similarity between the incompressible and compressible turbulence field. In turn, this lends credence to the assumption of the Morkovin hypothesis for the turbulence field near a wall.

A two-step process is used to verify these points. The first step is a comparison of the compressible turbulence field with an incompressible field at about the same Re_θ. To carry out this comparison, a reduced Re_θ, which is defined as the Re_θ calculated using fluid properties evaluated at the wall rather than in the freestream, is introduced. The symbol $(Re_\theta)_w$ is used to denote this Reynolds number. The Re_θ of the DNS data set is $\sim 5.4 \times 10^3$. On reduction, the $(Re_\theta)_w$ becomes 1.7×10^3. The incompressible data selected are the DNS data of Spalart[10] and the measurements of Karlsson and Johansson[11] with Re_θ of 1.41×10^3 and 2.42×10^3, respectively. Therefore, they bracket the $(Re_\theta)_w$ of the compressible DNS data. In the following comparisons of the turbulence statistics, the Reynolds numbers specified are the $(Re_\theta)_w$. The second step is a comparison of the model calculations with the DNS/experimental data for both compressible and incompressible flows. Because the incompressible flow cases have already been calculated,[17] their results are used in the present analysis. Thus, the ability of the model to predict incompressible and compressible near-wall turbulence can be analysed in detail as well.

A comparison of the mean velocity in the conventional law of the wall and the van Driest law-of-the-wall plot is shown in Figs. 1a and 1b. Here, y^+ also denotes y_w^+ for compressible flows. In Fig. 1a, three sets of data and calculations are plotted. For incompressible flow, the calculations are in good agreement with DNS data in the sublayer, the buffer, and the log-law regions. The agreement extends to $y^+ \approx 200$. In the log-law region, the model calculations

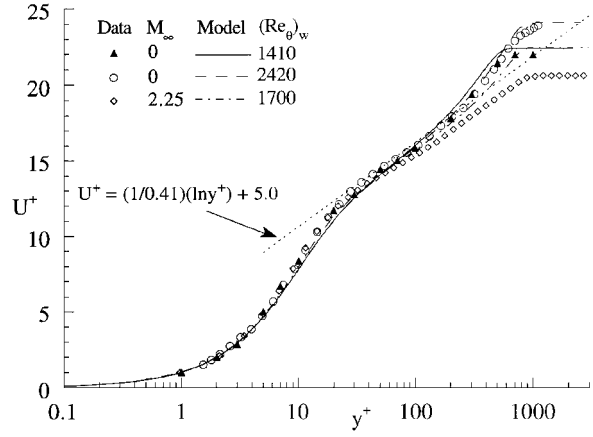

Fig. 1a Comparison of the U^+ behavior for incompressible and compressible flows.

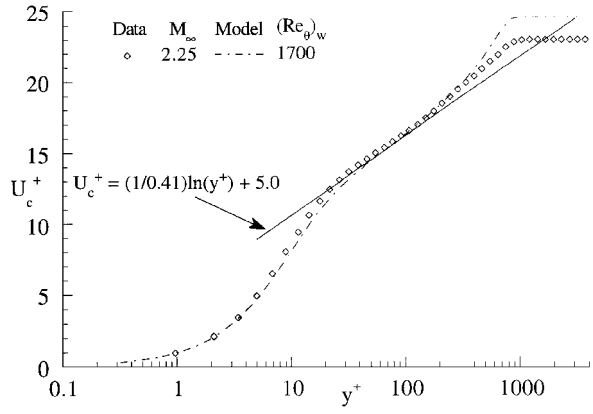

Fig. 1b Comparison of the U_c^+ behavior for compressible flows.

and the incompressible flow data yield a $\kappa = 0.41$. For compressible flow, the calculations are in good agreement with DNS data only in the sublayer and buffer regions. Agreement in the log layer extends only to $y^+ \approx 100$. Thereafter, the DNS data are consistently lower than the calculation. This gives rise to different κ for the log law; for the DNS data $\kappa = 0.426$ is determined, whereas $\kappa = 0.41$ is obtained for the model calculations. Up to $y^+ \approx 60$, the incompressible and compressible data and calculations are essentially identical. Therefore, they show that inner layer similarity is still valid for compressible boundary layers. The van Driest plots are shown in Fig. 1b; only the compressible DNS data and the model calculations are plotted. It can be seen that the predictions are in close agreement with the DNS data and κ_c is determined to be 0.41 for both DNS data and model calculations. The intercept B_c thus obtained is found to be about 5.0 also. This supports the use of a van Driest transformation for compressible boundary layers with adiabatic wall boundary condition at the M_∞ and Re_θ considered.

The plots of u', v', and w' are shown in Figs. 2a–2c, respectively. They are plotted in semilog form to illustrate inner layer similarity

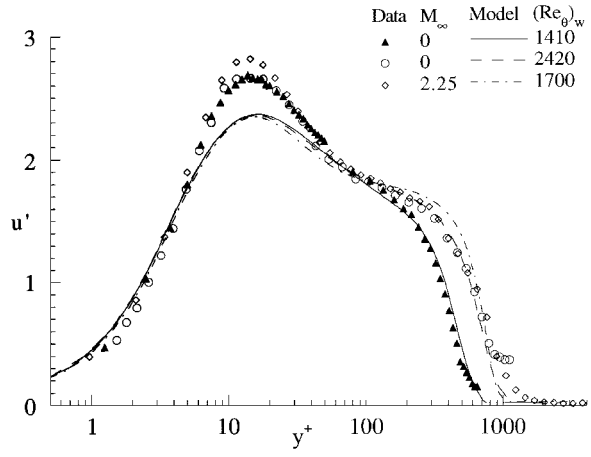

Fig. 2a Comparison of the u' behavior for incompressible and compressible flows.

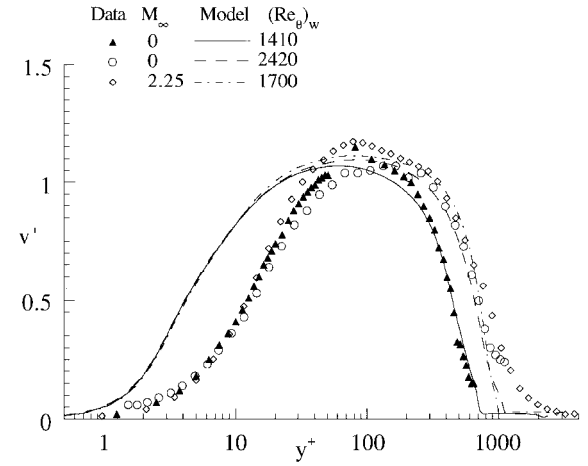

Fig. 2b Comparison of the v' behavior for incompressible and compressible flows.

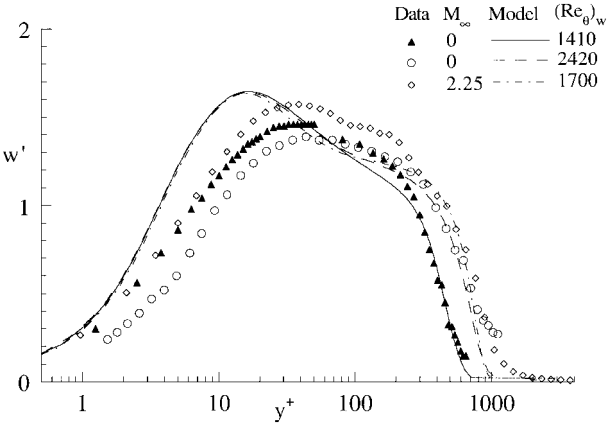

Fig. 2c Comparison of the w' behavior for incompressible and compressible flows.

or lack thereof. This way, the asymptotic behavior of the turbulence statistics can be clearly shown. The u' statistics of the incompressible boundary layers at two different Reynolds numbers are calculated correctly near the wall (Fig. 2a) but not the behavior of v' and w' (Figs. 2b and 2c). Similar trends are also observed for the compressible boundary layer. Note that the discrepancies shown in Figs. 2b and 2c for v' and w' are common for both incompressible and compressible flows and could be attributed to model deficiency. Inner layer similarity is displayed by the data for all turbulence statistics shown (Figs. 2a–2c). The exception is the experimentally measured w'. The reason for this discrepancy is not known. It cannot be due to measurement inaccuracy; otherwise, this would be more likely reflected in the measurements of v' rather than w' because the measurements of the wall normal component are known to be less accurate than the streamwise and transverse components for both hot-wire and laser Doppler anemometers. In the inner region, the compressible DNS data are essentially identical to its incompressible counterpart. The similarity region extends to $y^+ \approx 20$, depending on the statistics examined. Beyond this region, both data sets display the same trend even though they are not in quantitative agreement with each other. There is one difference, though, and that is the more prominent plateau and the higher peak.

In general, the peaks reached in the compressible statistics are higher than the incompressible ones. This is due to compressible heating of the fluid and is evident from the u', v', and w' difference between the compressible and incompressible data in the region $20 < y^+ < 1000$. The model calculations also show a similar heating effect in the v' component (Fig. 2b). However, the extent is very limited, and the intensity is much less, particularly around the peak region. Consequently, the peaks in the calculated turbulence statistics are lower than those shown in the DNS data. The heating effects are derived from the neglected term $\overline{p'u'_{i,i}}$ in Eqs. (6) and (7) and the terms $\bar{u}_i$, $\bar{\rho}\Pi^{dl}_{ij}$, and $\bar{\rho}M_{ij}$ in Eq. (7). Prominent in these neglected terms is $\overline{p'u'_{i,i}}$, which is identically zero for incompressible flow but finite for compressible flow. The term $u'_{i,i}$ is the divergence of the Reynolds fluctuating velocity and represents the volume change resulting from compressibility. Therefore, the term $\overline{p'u'_{i,i}}$ represents pressure dilatation resulting from compressible heating effects. It is obvious that the model, which is based on a set of simplified equations, fails to replicate the compressible heating effects correctly. If these effects are to be accounted for properly, most likely the neglected terms, such as $\overline{p'u'_{i,i}}$, $\bar{u}_i$, $\bar{\rho}\Pi^{dl}_{ij}$, $\bar{\rho}M_{ij}$, etc., have to be restored in Eq. (7). In spite of this discrepancy, it can be said that the assumption of dynamic similarity of the turbulence field between compressible and incompressible flows is still appropriate. Therefore, the Morkovin hypothesis can also be assumed to be approximately valid for the turbulence field, at least in the inner region, $0 < y^+ < 20$.

Recently, the work of Sarkar[40] and Simone et al.[41] suggested that compressibility effects distinct from the variation of mean density occur when the gradient Mach number M_g, defined with respect to the mean velocity gradient, a turbulence length scale, and the local speed of sound, is of order 1 and that M_g is small in the supersonic boundary layer but not in the supersonic shear layer. For compressible boundary layers, M_g can be written as $M_g = M_\infty (C_f/2)^{1/2}/\kappa$. The M_g thus calculated for the cases considered here are also listed in Table 1. It can be seen that $M_g = 0.17$ for the DNS case ($M_\infty = 2.25$), but it reaches 0.52 for the highly cooled case where $M_\infty = 8.18$. For the latter case, the maximum mean temperature $\tilde{\Theta}$ within the boundary layer is about five times that of the freestream temperature Θ_∞, whereas it is only about 2.5 times for the DNS case (see discussion in the following section). Therefore, the effect due to mean density variation will be proportionally larger for the highly cooled case. Even though $M_g = 0.52$, it is expected that the stabilizing effect of compressibility will still be relatively small compared with the mean density effects. Together, these results, plus the mean field comparisons to be shown later, indicate that, for the cases considered here, compressibility effects are mainly derived from the variation of mean density, or the stabilizing effect of compressibility on turbulence is not apparent. In other words, the Morkovin hypothesis could still be considered valid for the cases calculated here.

The compressible DNS uv^+ data (Fig. 3) show inner layer similarity with the incompressible counterpart up to $y^+ \sim 20$. However, consistent with the other turbulent normal stress comparisons, the peak is higher than the corresponding incompressible peak value; in a certain region its value exceeds unity by about 1.5%. This suggests that the actual peak value for uv^+ is close to unity, and the results computed here represent slight inaccuracies in the simulation resolution or in the postprocessing of scaling quantities such as u_τ. Model calculations of uv^+ follow the DNS data very closely (Fig. 3) except in a region around the peak. This discrepancy can again be attributed to the inability of the model to account for the compressible heating effects correctly. The model calculations of the incompressible k^+

Table 2 Comparisons of the asymptotic behavior of the turbulence statistics near a wall

	Data					Model calculations				
Re_θ	$a_{uv}/a_u a_v$	a_k	a_u^2/a_k	$(a_v^2/a_k)\times 10^3$	a_w^2/a_k	$a_{uv}/a_u a_v$	a_k	a_u^2/a_k	$(a_v^2/a_k)\times 10^3$	a_w^2/a_k
1.41×10^3	0.27	0.13	1.43	0.8	0.58	0.057	0.144	1.36	21.4	0.64
2.42×10^3	0.33	0.13	1.72	2.0	0.31	0.068	0.148	1.36	21.3	0.64
1.7×10^3	0.37	0.11	1.47	0.45	0.52	0.13	0.133	1.30	13.8	0.60

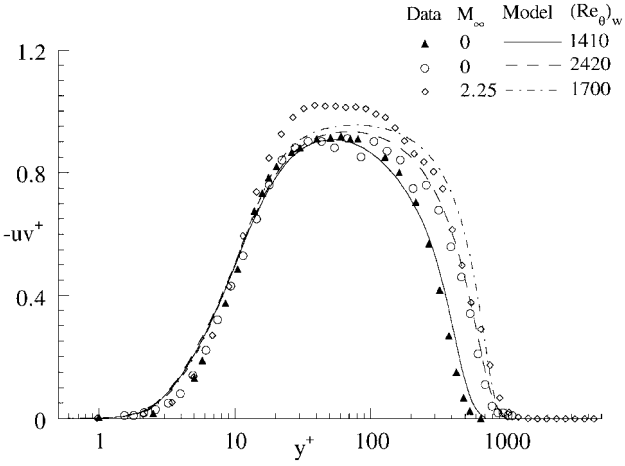

Fig. 3 Comparison of the $-uv^+$ behavior for incompressible and compressible flows.

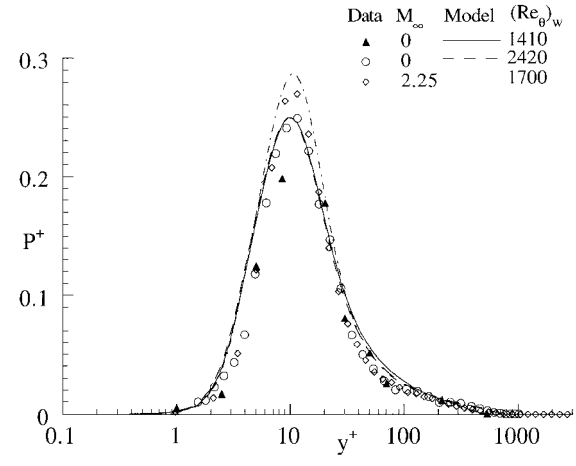

Fig. 5 Comparison of the P^+ behavior for incompressible and compressible flows.

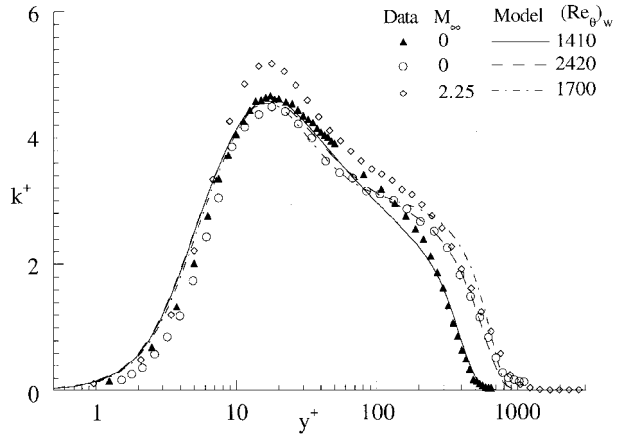

Fig. 4 Comparison of the k^+ behavior for incompressible and compressible flows.

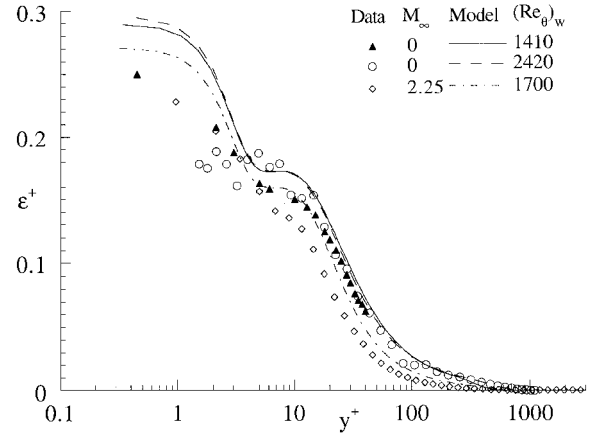

Fig. 6 Comparison of the ε^+ behavior for incompressible and compressible flows.

exhibit a plateau and are in agreement with the incompressible DNS and experimental data (Fig. 4). On the other hand, the compressible DNS result for k^+ shows a much higher peak and a less prominent plateau. The disappearance of the plateau in the DNS data is probably due to compressible heating, which tends to promote turbulent mixing. Because the model calculation cannot fully replicate this effect, the predictions are not in good agreement with DNS data in this region. Inner layer similarity is again displayed by all data and calculations up to $y^+ \sim 20$.

The asymptotic behavior of the turbulence statistics as given by the leading coefficients in Eq. (20) is also examined. These coefficients are determined from the data and the model calculations and are listed in Table 2 for comparison. It can be seen that the coefficients for the compressible case are essentially the same as those for the incompressible cases. Also, with the exception of the prediction of a_v, the other calculated results are in fair agreement with the data for both compressible and incompressible boundary-layer flows. In spite of the poor agreement shown in Fig. 2c for w', the calculated a_w is in fair agreement with the data. This result is consistent because a_w is determined using values limited to $y^+ < 3$, whereas the noted discrepancy starts from this point. Further, the discrepancy between the calculated value of $a_{uv}/a_u a_v$ and the data is due mainly to the incorrect predictions of a_v rather than a_{uv}. As expected, the asymptotic behavior as defined by Eq. (20) and the ratios $k^+/\varepsilon^+ y^{+2} = \frac{1}{2}$ and $(a_u^2 + a_v^2 + a_w^2)/a_k = 2$ are again calculated correctly (Table 2). This is evident from the calculated compressible ε_w^+, which is 0.270 compared with an $a_k = 0.133$.

The production and dissipation of k are shown in Figs. 5 and 6. These quantities are normalized by u_τ and the fluid properties evaluated at the wall. In Fig. 5, consistent with the thin shear layer approximations, only $P^+ = -uv^+(\partial U^+/\partial y^+)$ is shown. For incompressible flows, the P^+ distributions should collapse into a single curve,[16] and this has been further verified over a wide range of Reynolds numbers.[20] Also, the location and the peak of the maximum production rate do not vary with Reynolds number. For incompressible flows,[20] it can be shown that the peak asymptotes to 0.25 as $Re \to \infty$. The model calculations and DNS data of the compressible flow case examined are in good agreement with each other and display the same behavior as the incompressible flow data and calculations. However, the peak is greater than 0.25, a consequence of the higher peak reached in the compressible uv^+ distribution (Fig. 3). This peak is also predicted by the near-wall Reynolds-stress model.

The good agreement between the predicted P^+ and DNS data is a consequence of the underprediction of uv^+ and the overprediction of the mean velocity gradient. The latter fact is supported by the predicted κ of 0.41 compared with the DNS value of $\kappa = 0.426$. The location of the maximum production rate is in good agreement with its incompressible counterpart and occurs at $y^+ \approx 10$. This result lends further credence to the Morkovin hypothesis for the turbulence field.

On the other hand, the DNS ε_s is not in complete agreement with the incompresible flow data (Fig. 6) as in the P^+ comparison. The ε_s distribution does not display a plateau and is lower than the incompressible ε. Taking ε_c into account fails to improve the agreement by much because it is very small compared with ε_s. Both the incompressible and compressible model calculations and the incompressible data display such a plateau in the region $7 < y^+ < 12$. This region approximately corresponds to the location of the P^+ maximum shown in Fig. 5. In spite of these differences, the compressible DNS data for ε^+ show a rise to a wall value of 0.227 and are very close to those given by the incompressible flow. The compressible part of the dissipation rate has very little effect on the predictions of other turbulence statistics; therefore, its neglect is quite justified in compressible turbulence modeling applicable to flows in the parameter range studied here.

Mean Field Validation

The selected mean flow results are compared in the following manner. Plots of the conventional law of the wall and the van Driest law of the wall are shown in parts a and b of each figure. In the van Driest plots, Eq. (19) is also shown for comparison so that the agreement or lack thereof between Eq. (19) and measurements can be clearly illustrated. The mean temperatures for the adiabatic wall cases are not compared because they are inferred from the mean velocity measurements. However, the mean temperatures of

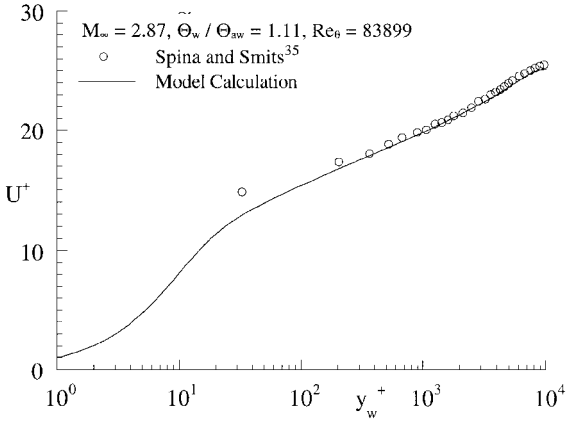

Fig. 7a Comparison of the conventional law-of-the-wall plot with measurements.

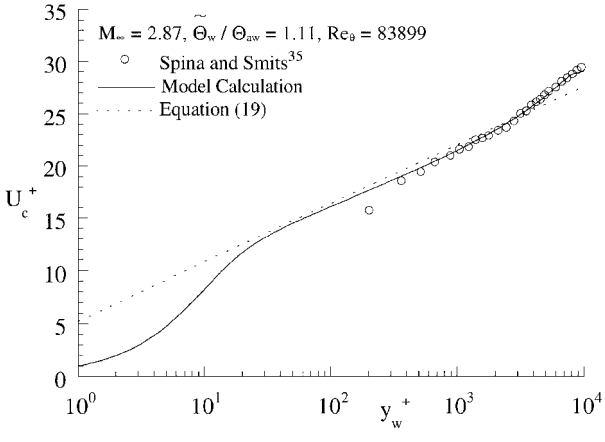

Fig. 7b Comparison of the van Driest law-of-the-wall plot with measurements.

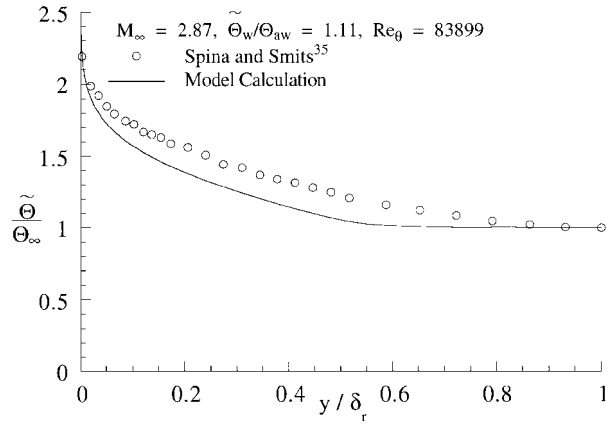

Fig. 8 Comparison of the mean temperature with measurements in linear plot.

the heated and cooled wall cases are measured independently and are compared in linear plots with model calculations. In the linear plots, the mean temperature is plotted vs y/δ_r, where δ_r is the boundary-layer thickness determined from either the measurements or the calculations.

The measured and calculated velocity profiles of the heated wall case[35] are shown in Figs. 7a and 7b, and the C_f, κ, and κ_c are compared in Table 1. The von Kármán constants are determined using Eqs. (18) and (19) and by following the procedure outlined in Ref. 37. It can be seen that the model prediction is in good agreement with the conventional as well as the van Driest law of the wall. As far as the prediction of C_f is concerned, the modeled result is within 5% of the measured C_f. The model prediction of the mean temperature is in error (Fig. 8). This could be due to the fact that a constant Pr_t is assumed. According to Sommer et al.,[42] the turbulent Prandtl number is not constant even for incompressible flow with heat transfer where the temperature difference is of the order of 20°C. Therefore, there is no good reason to expect the constant Pr_t assumption to be completely valid in this case. Sommer et al.[26,27] have applied their incompressible variable turbulent Prandtl number model[42] to calculate compressible flows using a two-equation model as well as a Reynolds-stress model, and slightly improved agreement with measurements was obtained compared with those given by the constant Pr_t assumption. Perhaps improved results could also be obtained with the present Reynolds-stress model if the variable Pr_t model[40] is used to model the turbulent heat flux. In terms of κ and κ_c, the agreement between calculations and measurements is fairly good, and for this wall heating case, κ and κ_c are determined to be quite different. Their values differ from 0.41; κ is more like 0.51, whereas κ_c is approximately 0.37 (Table 1). This means that the van Driest law of the wall is not quite applicable even for a compressible flow over a slightly heated wall at fairly low M_∞.

Three cases, ranging in M_∞ from 2.25 to 10.31, are calculated for the adiabatic wall boundary condition. Unlike the heated wall case, where $Re_\theta = 8.3899 \times 10^4$, the Reynolds number at the location where measurements are available varies from a low of 5.32×10^3 to a high of 1.5074×10^4. These values are listed in Table 1. The comparisons between model calculations and measurements for the $M_\infty = 10.31$ case[31] are given in Figs. 9a and 9b, whereas the calculated C_f, κ, and κ_c for all three cases are again listed in Table 1 for comparisons with measurements. At low M_∞ (Fig. 1), the model calculations are essentially identical, and the κ and κ_c thus determined are about the same. The calculated C_f for the $M_\infty = 2.25$ case is smaller than the DNS data by about 5%. This amount of discrepancy is consistent with the agreement shown in the mean velocity plots (Figs. 1a and 1b). On the other hand, the calculations are in good agreement with data for the $M_\infty = 4.54$ case (Table 1). At $M_\infty = 10.31$, the conventional law-of-the-wall plots of the model calculations are not in agreement with measurements (Fig. 9a). This is due mainly to an underestimation of C_f, which is in error by about 17%. When the comparisons are made in linear and van Driest plots (Fig. 9b), the calculations correlate well with measurements. According to Huang et al.,[28] this underestimation could be attributed

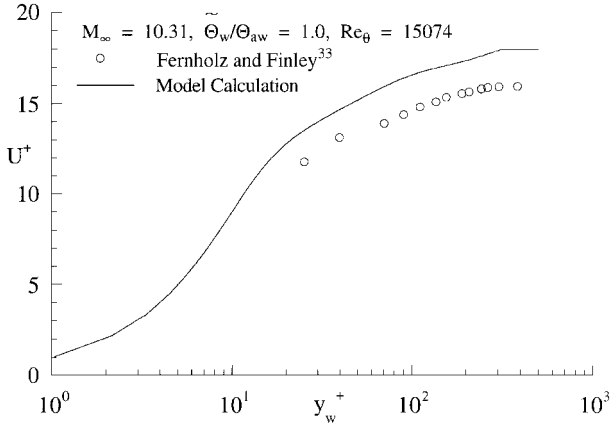

Fig. 9a Comparison of the conventional law-of-the-wall plot with measurements.

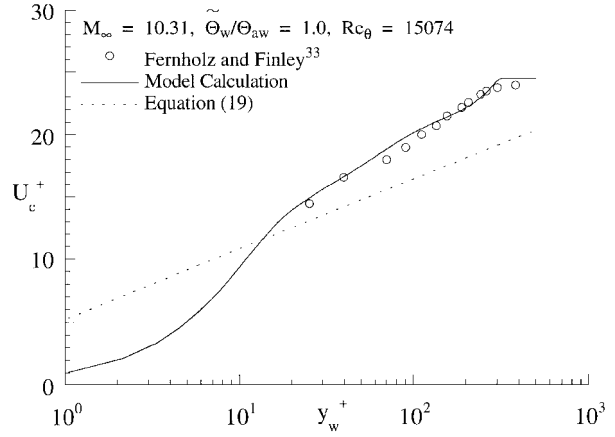

Fig. 9b Comparison of the van Driest law-of-the-wall plot with measurements.

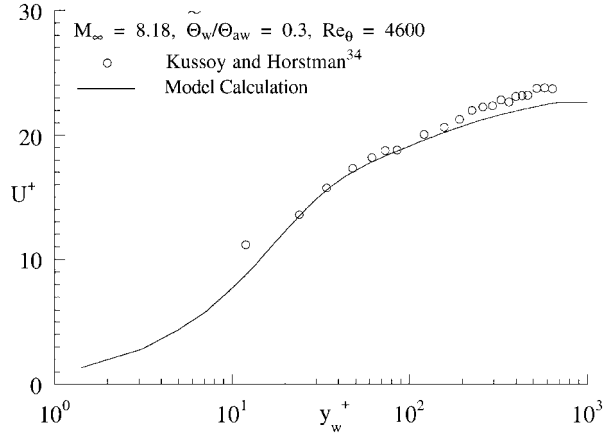

Fig. 10a Comparison of the conventional law-of-the-wall plot with measurements.

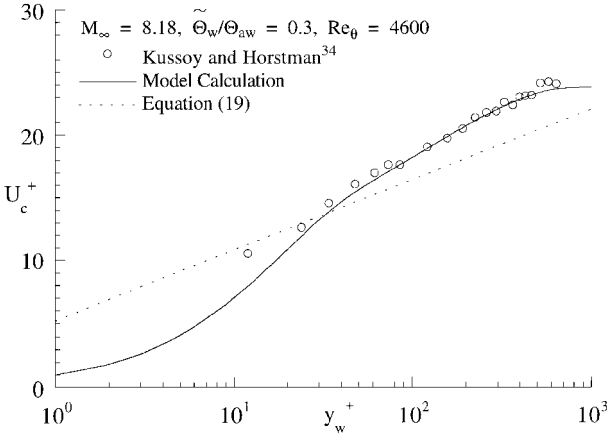

Fig. 10b Comparison of the van Driest law-of-the-wall plot with measurements.

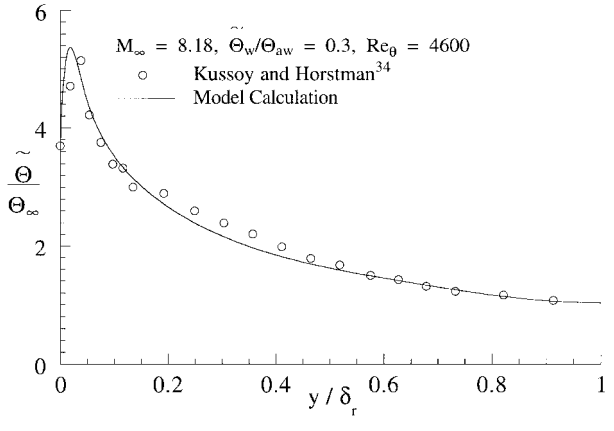

Fig. 11 Comparison of the mean temperature with measurements in linear plot.

to low-Reynolds-number effects on the wake flow not being taken into account properly. If they were taken into account, the wall shear would have been calculated correctly.[28] The discrepancy noted in Fig. 9a could also be attributed to the neglect of the compressible term in the modeled equations and the assumption of a constant Pr_t, which may not be valid at these high M_∞. Because Pr_t is known to increase sharply as a wall is approached,[26] the incorrect estimate of C_f by the near-wall Reynolds-stress model could be partially attributed to the constant Pr_t assumption. At this M_∞, κ_c is significantly different from 0.41. Consequently, the data points do not follow the van Driest law of the wall (Fig. 9b). On the other hand, the conventional law of the wall with a κ parametric in M_τ can still be used to correlate the mean velocity. The κ thus determined is substantially larger than 0.41 (Table 1). Based on these comparisons, it can be said that the van Driest law of the wall is perhaps most valid for compressible flows over an adiabatic wall with low-to-medium M_∞.

Two flow cases covering medium-to-high M_∞ and near adiabatic wall to highly cooled wall boundary conditions are also calculated. One is the slightly cooled wall case[32] with $M_\infty = 5.29$ and $\tilde{\Theta}_w/\Theta_{aw} = 0.92$, and another is the highly cooled wall case[34] with $M_\infty = 8.18$ and $\tilde{\Theta}_w/\Theta_{aw} = 0.30$. The model calculations are in fair agreement with measurements (Figs. 10a and 10b) even though C_f is underpredicted by as much as 14% in the $M_\infty = 5.29$ case and slightly overestimated for the $M_\infty = 8.18$ case. In view of this, the semilog plots of the mean velocity lie above the measured data for the $M_\infty = 5.29$ case and below the measured data for the $M_\infty = 8.18$ case (Fig. 10a). Again, the mean velocities in the van Driest plots are in good agreement with measurements (Fig. 10b). The mean temperature prediction, on the other hand, correlates very well with measurements (Fig. 11), and the agreement is even better than that shown for the heated wall case in Fig. 8. Perhaps relaxing the assumption of a constant Pr_t could improve the prediction of C_f. The various κ_c determined from the measurements deviate significantly from 0.41 (Table 1). Even at $\tilde{\Theta}_w/\Theta_{aw} = 0.92$, κ_c is found to be about 0.34. In other words, the van Driest law of the wall cannot suitably describe the log-law region if κ_c is taken to be 0.41. The conventional law of the wall shows that κ is also dependent on the total heat flux, and hence it should vary as the wall temperature ratio decreases. Both the data and the calculations show that κ is indeed decreasing as M_∞ increases and the wall temperature ratio decreases. The errors in the predicted κ are larger than the other cases, but this could be due to the assumption of a constant Pr_t which is more applicable to flows over an adiabatic wall than to flows over a cooled wall.

Finally, the asymptotic values of $k^+/\varepsilon^+ y^{+2}$ and $(a_u^2 + a_v^2 + a_w^2)/a_k$ are calculated to be $\frac{1}{2}$ and 2, respectively, thus indicating that the

asymptotic analyses carried out for incompressible flows are equally applicable for compressible flows, even at these high M_∞.

Conclusions

A near-wall Reynolds-stress closure based on the SSG pressure-strain model was extended to calculate turbulent compressible flows. The extension was carried out by invoking the Morkovin hypothesis. Although the Morkovin hypothesis has been invoked before and has proven to be valid for the mean field, its suitability for the turbulence field has not been demonstrated. With data from the direct numerical simulation of a flat plate boundary layer on an adiabatic wall at $M_\infty = 2.25$, detailed turbulence statistics are now available for assessing the validity of the Morkovin hypothesis for the turbulence field. This has been carried out together with a detailed validation of the mean field using experimental data sets that were obtained from adiabatic and constant-temperature wall boundary conditions and with M_∞ varying from 2.87 to 10.31. Furthermore, a comparison of the compressible turbulence statistics with their corresponding quantities obtained in two incompressible flat plate boundary layers at comparable Reynolds numbers is carried out. The results show that, in the inner region, the compressible turbulence statistics are essentially identical to their corresponding incompressible ones. They differ only in the buffer region where compressible heating promotes turbulence, thus giving rise to more intense turbulent mixing. The model predictions of the mean field are in good agreement with measurements, whereas the predictions of the compressible turbulence statistics are very similar to the model predictions of the incompressible behavior. Therefore, there is indeed a dynamic similarity of the incompressible and compressible mean and turbulence field, and the Morkovin hypothesis is valid for both fields. The validity of the Morkovin hypothesis rests on the assumption that the gradient Mach number in the boundary layer is small.

Altogether, these results show that the van Driest law of the wall is essentially valid for compressible flows over an adiabatic wall with fairly low M_∞. Wall cooling and high freestream Mach numbers have the same effect on κ_c. Both tend to reduce the value of κ_c to one that is substantially below 0.41. On the other hand, κ is determined to be 0.41 from the conventional law-of-the-wall plots for compressible flows over an adiabatic wall up to $M_\infty = 4.54$. As predicted by Eq. (18), κ is parametric in M_τ, B_q, and γ. The present analysis shows that this is indeed the case. This is also true for κ_c. The behavior of κ and κ_c with M_∞ and $\tilde{\Theta}_w/\Theta_{aw}$ is reproduced fairly well. Finally, the predictive capability of the near-wall Reynolds-stress model is achieved without having to alter any of the model constants.

Acknowledgments

Part of this work was carried out at Arizona State University with support from NASA Langley Research Center under Grant NAG-1-1080. The paper was completed after the first author moved to the Hong Kong Polytechnic University. Therefore, support given by these two organizations is gratefully acknowledged.

References

[1]So, R. M. C., Lai, Y. G., Zhang, H. S., and Hwang, B. C., "Second-Order Near-Wall Turbulence Closures: A Review," *AIAA Journal*, Vol. 29, 1991, pp. 1819–1835.

[2]Launder, B. C., Reece, G. J., and Rodi, W., "Progress in the Development of a Reynolds-Stress Turbulence Closure," *Journal of Fluid Mechanics*, Vol. 68, 1975, pp. 537–566.

[3]Hanjalic, K., and Launder, B. E., "Contribution Towards a Reynolds-Stress Closure for Low-Reynolds-Number Turbulence," *Journal of Fluid Mechanics*, Vol. 74, 1976, pp. 593–610.

[4]Prud'homme, M., and Elghobashi, S., "Prediction of Wall-Bounded Turbulent Flows with an Improved Version of a Reynolds-Stress Model," *Proceedings of the 4th Symposium on Turbulent Shear Flows*, 1983 (Paper 1.2).

[5]So, R. M. C., and Yoo, G. J., "On the Modeling of Low-Reynolds-Number Turbulence," NASA CR-3994, 1986.

[6]Shima, N., "A Reynolds-Stress Model for Near-Wall and Low-Reynolds-Number Regions," *Journal of Fluids Engineering*, Vol. 110, 1988, pp. 38–44.

[7]Launder, B. E., and Shima, N., "Second-Moment Closure for the Near-Wall Sublayer: Development and Application," *AIAA Journal*, Vol. 27, 1989, pp. 1319–1325.

[8]Lai, Y. G., and So, R. M. C., "On Near-Wall Turbulent Flow Modeling," *Journal of Fluid Mechanics*, Vol. 221, 1990, pp. 641–673.

[9]Kim, J., Moin, P., and Moser, R. D., "Turbulence Statistics in Fully Developed Channel Flow at Low Reynolds Number," *Journal of Fluid Mechanics*, Vol. 177, 1987, pp. 133–186.

[10]Spalart, P. R., "Direct Simulation of a Turbulent Boundary Layer up to $R_\theta = 1410$," *Journal of Fluid Mechanics*, Vol. 187, 1988, pp. 61–98.

[11]Karlsson, R. I., and Johansson, T. G., "LDV Measurements of Higher Order Moments of Velocity Fluctuations in a Turbulent Boundary Layer," *Laser Anemometry in Fluid Mechanics*, edited by D. F. G. Durao et al., Ladoan—Instituto Superior Tecnico, Portugal, 1988, pp. 273–289.

[12]Alfredsson, P. H., Johansson, A. V., Haritonidis, J. H., and Eckelmann, H., "The Fluctuating Wall Shear Stress and the Velocity Field in the Viscous Sublayer," *Physics of Fluids*, Vol. 31, 1988, pp. 1026–1033.

[13]Wei, T., and Willmarth, W. W., "Reynolds-Number Effects on the Structure of a Turbulent Channel Flow," *Journal of Fluid Mechanics*, Vol. 204, 1989, pp. 57–95.

[14]Nishino, K., and Kasagi, N., "Turbulence Statistics Measurements in a Two-Dimensional Channel Flow Using a Three-Dimensional Particle Tracking Velocimeter," *Proceedings of the 7th Symposium on Turbulent Shear Flows*, 1989 (Paper 22).

[15]Durst, F., Jovanovic, J., and Sender, J., "Detailed Measurements of the Near Wall Region of Turbulent Pipe Flows," *Proceedings of the 9th Symposium on Turbulent Shear Flows*, 1993 (Paper 2.2).

[16]Bandyopadhyay, P. R., and Gad-el-Hak, M., "Reynolds Number Effects in Wall-Bounded Turbulent Flows," U.S. Naval Undersea Warfare Center Div., NUWC-NPT TR 10296, Newport, RI, 1994.

[17]So, R. M. C., Aksoy, H., Sommer, T. P., and Yuan, S. P., "Development of a Near-Wall Reynolds-Stress Closure Based on the SSG Model for the Pressure Strain," NASA CR-4618, 1994.

[18]Speziale, C. G., Sarkar, S., and Gatski, T. B., "Modeling the Pressure-Strain Correlation of Turbulence: An Invariant Dynamical Systems Approach," *Journal of Fluid Mechanics*, Vol. 227, 1991, pp. 245–272.

[19]Demuren, A. O., and Sarkar, S., "Perspective: Systematic Study of Reynolds Stress Closure Models in the Computations of Plane Channel Flows," *Journal of Fluids Engineering*, Vol. 115, 1993, pp. 5–12.

[20]So, R. M. C., Aksoy, H., Sommer, T. P., and Yuan, S. P., "Modeling Reynolds Number Effects in Wall-Bounded Turbulent Flows," *Journal of Fluids Engineering*, Vol. 118, 1996, pp. 260–267.

[21]Morkovin, M., "Effects of Compressibility on Turbulent Flows," *Mecanique de la Turbulence*, edited by A. Favre, Gordon and Breach, New York, 1962, pp. 367–380.

[22]Sarkar, S., Erlebacher, G., Hussaini, M. Y., and Kreiss, H. O., "The Analysis and Modeling of Dilatational Terms in Compressible Turbulence," *Journal of Fluid Mechanics*, Vol. 227, 1991, pp. 473–493.

[23]Speziale, C. G., and Sarkar, S., "Second-Order Closure Models for Supersonic Turbulent Flows," AIAA Paper 91-0217, 1991.

[24]Zhang, H. S., So, R. M. C., Speziale, C. G., and Lai, Y. G., "A Near-Wall Two-Equation Model for Compressible Turbulent Flows," *AIAA Journal*, Vol. 31, 1993, pp. 196–199.

[25]Zhang, H. S., So, R. M. C., Gatski, T. B., and Speziale, C. G., "A Near-Wall Second-Order Closure for Compressible Turbulent Flows," *Near-Wall Turbulent Flows*, edited by R. M. C. So, C. G. Speziale, and B. E. Launder, Elsevier, Amsterdam, 1993, pp. 209–218.

[26]Sommer, T. P., So, R. M. C., and Zhang, H. S., "A Near-Wall Variable-Prandtl-Number Turbulence Model for Compressible Flows," *AIAA Journal*, Vol. 31, No. 1, 1993, pp. 27–35.

[27]Sommer, T. P., So, R. M. C., and Zhang, H. S., "Supersonic Flow Calculations Using a Reynolds-Stress and a Thermal Eddy Diffusivity Turbulence Model," *Journal of Fluids Engineering*, Vol. 116, 1994, pp. 469–476.

[28]Huang, P. G., Bradshaw, P., and Coakley, T. J., "A Skin Friction and Velocity Profile Family for Compressible Turbulent Boundary Layers," *AIAA Journal*, Vol. 31, 1993, pp. 1600–1604.

[29]Rai, M. M., Gatski, T. B., and Erlebacher, G., "Direct Simulations of Spatially Evolving Supersonic Turbulent Boundary Layers" (submitted for publication).

[30]Coles, D., "Measurements of Turbulent Friction on a Smooth Flat Plate in Supersonic Flow," *Journal of the Aeronautical Sciences*, Vol. 21, No. 6, 1954, pp. 433–448.

[31]Watson, R. D., Harris, J. E., and Anders, J. B., "Measurements in a Transitional/Turbulent Mach 10 Boundary Layer at High Reynolds Numbers," AIAA Paper 73-165, 1973.

[32]Winkler, E. M., and Cha, M. H., "Investigation of Flat Plate Hypersonic Turbulent Boundary Layers with Heat Transfer at a Mach Number of 5.2," NOL NAVORD Rept. 6631, 1959.

[33]Fernholz, H. H., and Finley, P. J., "A Critical Compilation of Compressible Turbulent Boundary Layer Data," AGARDograph 223, 1977.

[34]Kussoy, M. I., and Horstman, K. C., "Documentation of Two- and Three-Dimensional Shock-Wave Turbulent-Boundary-Layer Interaction Flows at Mach 8.2," NASA TM-103838, 1991.

[35]Spina, E. F., and Smits, A. J., "Organized Structures in a Compressible, Turbulent Boundary Layer," *Journal of Fluid Mechanics*, Vol. 182, 1987, pp. 85–109.

[36] Anderson, E. C., and Lewis, C. H., "Laminar or Turbulent Boundary-Layer Flows of Perfect Gases or Reacting Gas Mixtures in Chemical Equilibrium," NASA CR-1893, 1971.

[37] So, R. M. C., Zhang, H. S., Gatski, T. B., and Speziale, C. G., "On Logarithmic Laws for Compressible Turbulent Boundary Layers," *AIAA Journal*, Vol. 32, 1994, pp. 2162–2168.

[38] van Driest, E. R., "Turbulent Boundary Layer in Compressible Fluids," *Journal of the Aeronautical Sciences*, Vol. 18, 1951, pp. 145–160.

[39] Millikan, C. B., "A Critical Discussion of Turbulent Flow in Channels and Circular Pipes," *Proceedings of the Fifth International Congress on Applied Mechanics*, Wiley, New York, 1939, pp. 386–392.

[40] Sarkar, S., "The Stabilizing Effect of Compressibility in Turbulent Shear Flow," *Journal of Fluid Mechanics*, Vol. 282, 1995, pp. 163–186.

[41] Simone, A., Coleman, G. N., and Cambon, C., "The Effect of Compressibility on Turbulent Shear Flow: A Rapid-Distortion-Theory and Direct-Numerical-Simulation Study," *Journal of Fluid Mechanics*, Vol. 330, 1997, pp. 307–338.

[42] Sommer, T. P., So, R. M. C., and Lai, Y. G., "A Near-Wall Two-Equation Model for Turbulent Heat Fluxes," *International Journal of Heat and Mass Transfer*, Vol. 35, 1992, pp. 3375–3387.

C. G. Speziale
Associate Editor

View publication stats